The Meteorological Magazine

June 1991

'Wet' stack plume analysis
Observations in climate study
L.G. Groves Awards

Met.O.998 Vol. 120 No. 1427

The Meteorological Magazine

June 1991
Vol. 120 No. 1427

551.551.8:628.53

An analysis of a 'wet' stack plume

F.B. Smith
Meteorological Office, Bracknell

Summary

How to calculate the visible length and ground-level concentrations resulting from a wet polluted plume emanating from an elevated stack is illustrated. In this example the stack is assumed to be on the outskirts of a fictitious town called Midville. It operates only during daytime, on a small slope within a housing area — typical of many such installations.

1. Introduction

It is assumed that an authority in Midville (somewhere in the Midlands of England) is proposing to build a new municipal incinerator with a stack for waste gases. The gases will contain sufficient water vapour to form a visible condensed plume which will be of potential concern to the local inhabitants.

The aims of the analysis in this paper can be summarized as:

(a) To determine the visible length of the plume in different weather conditions. The higher the humidity of the ambient air and the lower its temperature, the more slowly do the fine drops in the stack plume evaporate. Wind speed is also important since the stronger the wind the sooner, in terms of downwind distance, does the plume evaporate.

(b) To determine the maximum ground-level concentration of each significant pollutant contained in the plume, as measured over several minutes — say 10 minutes, wherever it may occur, as a function of stack height and weather conditions.

(c) To determine where these maximum concenations occur.

(d) To determine whether or not any surrounding houses are at risk from the effluent gases and what remedial action needs to be taken.

2. A list of the basic parameters

Values of the key parameters will be given the following values by way of illustration:

The temperature of the effluent gases at the stack top = 140 °C.
The efflux velocity (determined by a fan) = 15 m s^{-1}.
Maximum gas flow rate = 600 N m h^{-1}.
Internal stack diameter = 370 mm.
Water mixing ratio at the stack top = 0.3.

The stack height can be chosen to give least nuisance, remembering that local inhabitants will tend to object to a tall unsightly stack even more than to the occasional odour. Calculations are made for 16 m, 20 m and 23 m. Extreme values of 10 m and 30 m are also considered.

The effluent gas will contain a mixture of substances including hydrochloric acid (HCl), sulphur dioxide (SO_2), nitrogen oxides (NO_x) and carbon monoxide (CO). The assumed emission rates are: HCl 300 g h^{-1}, $SO_2/NO_x/CO$ 600 g h^{-1}.

3. The visible length of the plume

The gases rising up the stack contain a considerable amount of water which rapidly condenses on leaving the stack, giving a visible plume. As the plume broadens by turbulent mixing with the environmental air, drier and

colder air is mixed with the moist, stack air. This cools the plume, tending to retard its evaporation, but also dries it. How long the plume remains visible before this drying-out process results in total evaporation depends on the temperature and humidity of the environmental air. It also depends on the amount of natural turbulence in the air, which in turn depends on the stability of the lower atmosphere. The more stably stratified the air becomes, the lower is the level of turbulence and the slower the drying out of the plume.

The equations governing this process are now set out:

Let a = the emission of air = $1.67 \times 0.00127 \times 10^6$ g s^{-1} = 2.12×10^3 g s^{-1}, and

b = the emission of water = $0.3 \times 2.12 \times 10^3 = 0.64 \times 10^3$ g s^{-1}.

Define s = moisture content of the environmental air as a mixing ratio in g g^{-1}.

The total water emission is thus $(b + as)$ g s^{-1}, and the total dry air emission is $(1-s)a$ g s^{-1}.

The specific heat of air at constant pressure = 0.24, and that of water vapour = 0.48.

If, at a distance x downwind of the stack, the mass of entrained environmental air = m g, if T_f = the exit gas temperature = 140 °C, T_a = the temperature of the environmental air, T = the temperature of the plume at x, and S = the mixing ratio of the plume at x, then:

H_f = heat content of the flue gases = $(0.24(1-s)a + 0.48(b + sa))T_f$, where $a = 2120$, $b = 640$, and $T_f = 140$.

W_f = the water content of the flue gases = $(b + sa)$.

H_e = the heat content of the entrained air = $(0.24(1-s)m + 0.48\,sm)T_a$.

W_e = the water content of the entrained air = sm (which is a function of s and x).

H_p = the heat content of the plume = $T(0.24(1-s)(a+m) + 0.48(b + sa + sm))$.

W_p = the water content of the plume = $(a + b + m)S$.

Now $H_p = H_f + H_e$, so that $((1+s)a + 2b)(T_f - T) = (1+s)m(T - T_a)$.

Similarly $W_p = W_f + W_e$, so that $(a+b)(S_f - S) = m(S - s)$, where S_f is the water content of the flue gas = 0.3.

If we eliminate m from these two equations we arrive at the 'Mixing Curve' equation:

$$\frac{(1+s)a + 2b}{a+b}\left(\frac{T_f - T}{S_f - S}\right) = (1+s)\left(\frac{T - T_a}{S - s}\right).$$

Now after some mixing has occurred, certain simplifications can be made to this equation. We may assume that $T_f \gg T$, $S_f \gg S$ and $s \ll 1$. The Mixing Curve equation then simplifies to:

$$S - s = A(T - T_a)$$

where $A = (a+b)S_f/(a+2b)T_f = 0.00174$ if the values previously given are inserted. Strictly this value of A applies when $T = 0$. At $T = 10$ a more accurate value of A is 0.00187, and at $T = 20$ A is 0.00203. Now s is the mixing ratio of the environmental air and may be expressed as $rs_e(T_a)$, where s_e is the saturated mixing ratio at temperature T_a. If T_a is expressed in degrees Celsius then a good fit to $s_e(T_a)$ is given by:

$$s_e(T) = 10^{-3}(3.839 + 0.3008T + (0.00556T^2 + 0.0003587T^3)$$

r is the relative humidity (expressed as a fraction, not as a percentage).

The value of the plume temperature when the plume is on the point of evaporation is found by an iterative process. To begin, assume $T = T_a$. Insert this into the equation for s_e and find s_e. Insert this into the simplified mixing curve equation and find a new T. Repeat again and again until the solution converges to a constant value of T, and a corresponding value of S.

To find at what distance this occurs we must define how rapidly the plume broadens with distance. During the daytime, the plume will only persist a significant distance downwind in very humid conditions (when r is only a little less than 1). Such conditions occur in neutral stability conditions when the instantaneous plume width grows like:

$$R(x) = R(0) + 0.176x$$

where $R(x)$ is the radius (in metres) and x is the downwind distance, also in metres. The formula is consistent with the plume acting as a cone with a half-angle of about 10°. To find $R(0)$, we equate the volume flux emerging from the stack with the effective volume flux assuming the plume reaches its effective source height very rapidly and thereafter behaves like a horizontal plume being carried by the wind:

$$U\pi R^2(0) = \frac{a+b}{\rho}$$

where ρ = the air density = 1270 g m^{-3}.

Remembering that m is the mass of entrained air, an earlier equation gives

$$m = \frac{(a+b)(S_f - S)}{S - s} = \frac{0.3(a+b)}{0.0019(T - T_a)}$$

approximately. The total mass of the plume $M = m + (a+b) = 1270\pi R^2 U$. These equations relate the plume temperature T to distance x, and hence tells us the distance when the plume evaporates. These distances are given in Table I.

The figures summarize the results. Fig. 1 shows the saturation curve as a function of air temperature and its mixing ratio. The graph also shows a sample of 'mixing curve' lines which are virtually straight over the range of temperatures shown. Thus a plume from the stack emerging into an airstream whose temperature is 10 °C and relative humidity is 0.5 (as a fraction), evaporates when its temperature has fallen to 13 °C.

Table I. A table of the distances x, in metres, at which the plume from the stack evaporates, as a function of ambient temperature T_a, relative humidity r, and wind speed U (m s^{-1}) measured at 10 metres above ground

T_a	r	T_{evap}	$U=1$	$U=3$	$U=5$	$U=7$	$U=10$
0	0.4	1.45	44.9	25.9	20.1	17.0	14.2
	0.6	0.96	56.0	32.3	25.0	21.2	17.7
	0.8	0.48	81.1	46.8	36.3	30.6	25.6
	0.9	0.24	116.6	67.3	52.1	44.1	36.9
	0.95	0.12	166.8	96.3	74.6	63.0	52.7
	0.98	0.05	266.4	153.8	119.1	100.7	84.2
5	0.4	7.22	35.4	20.4	15.8	13.4	11.2
	0.6	6.47	44.4	25.7	19.9	16.8	14.1
	0.8	5.73	64.8	37.4	29.0	24.5	20.5
	0.9	5.36	93.7	54.1	41.9	35.4	29.6
	0.95	5.20	134.4	77.6	60.1	50.8	42.5
	0.98	5.07	215.3	124.3	96.3	81.4	68.1
10	0.4	13.53	27.2	15.7	12.2	10.3	8.6
	0.6	12.31	34.6	20.0	15.5	13.1	10.9
	0.8	11.14	51.1	29.5	22.9	19.3	16.2
	0.9	10.57	74.4	42.9	33.3	28.1	23.5
	0.95	10.28	107.2	61.9	48.0	40.5	33.9
	0.98	10.11	172.4	99.5	77.1	65.2	54.5
15	0.4	21.22	19.5	11.3	8.7	7.4	6.2
	0.6	18.93	25.6	14.8	11.4	9.7	8.1
	0.8	16.88	38.8	22.4	17.4	14.7	12.3
	0.9	15.92	57.3	33.1	25.6	21.6	18.1
	0.95	15.46	83.2	48.0	37.2	31.4	26.3
	0.98	15.18	134.5	77.7	60.2	50.8	42.5
20	0.8	23.52	27.3	15.7	12.2	10.3	8.6
	0.9	21.66	41.7	24.1	18.6	15.7	13.2
	0.95	20.81	61.7	35.6	27.6	23.3	19.5
	0.98	20.32	100.6	58.1	45.0	38.0	31.8
25	0.9	28.90	25.8	14.9	11.6	9.8	8.2
	0.95	26.70	41.3	23.8	18.5	15.6	13.1
	0.98	25.65	69.1	39.9	30.9	26.1	18.5

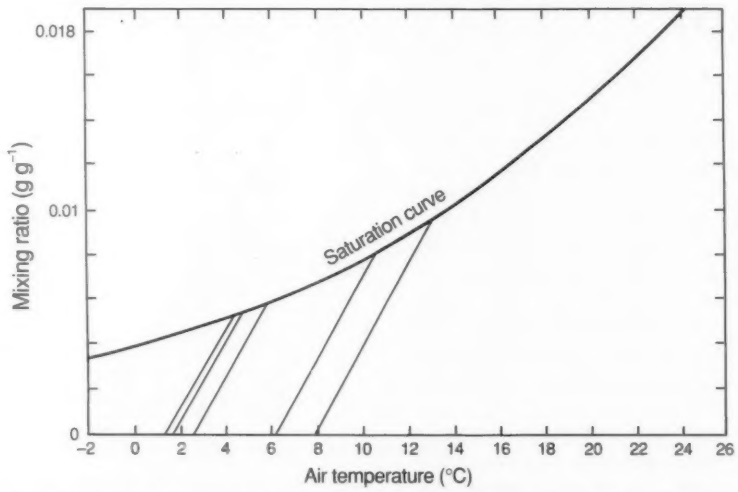

Figure 1. The saturation mixing ratio is a function of air temperature. Below the curve, the air is unsaturated. The nearly-straight lines running up to the saturation curve are the mixing curves for different ambient air conditions, but the same emerging plume conditions.

Fig. 2 shows how the maximum downwind extent of the visible plume varies with ambient air temperature, relative humidity and wind speed. It assumes near neutral stability conditions, which typically occur about 70% of the time in the United Kingdom. In unstable convective conditions, the plume would evaporate earlier whereas in stable conditions it would take longer. However, stable conditions are likely to occur during the daytime mainly at the very beginning and the very end of the working day when the stack is not operative. If stable conditions occur at other times (perhaps when milder air replaces bitterly cold air in winter) then the plume could be a temporary nuisance, and a case could be made for suspending incineration during such a period. During these times the plume length could be increased fivefold above the values given, although this is somewhat speculative.

As will be seen from the data, the visible length of the plume in neutral conditions exceeds 100 m in length only in very high humidity conditions and at low wind speeds and temperatures.

4. Maximum ground-level concentrations

Since concentrations are directly proportional to emissions, the calculations will be made using an emission rate $Q = 1\ g\ s^{-1}$. The ground-level concentrations are, however, not only dependent on source strength but on the effective height of the source, the wind speed and the stability of the air. The effective source height is defined as that height which, if the influences of gas temperature and efflux velocity were to be ignored, would give the same ground-level concentration pattern. The efflux gases are emitted within a vertical jet

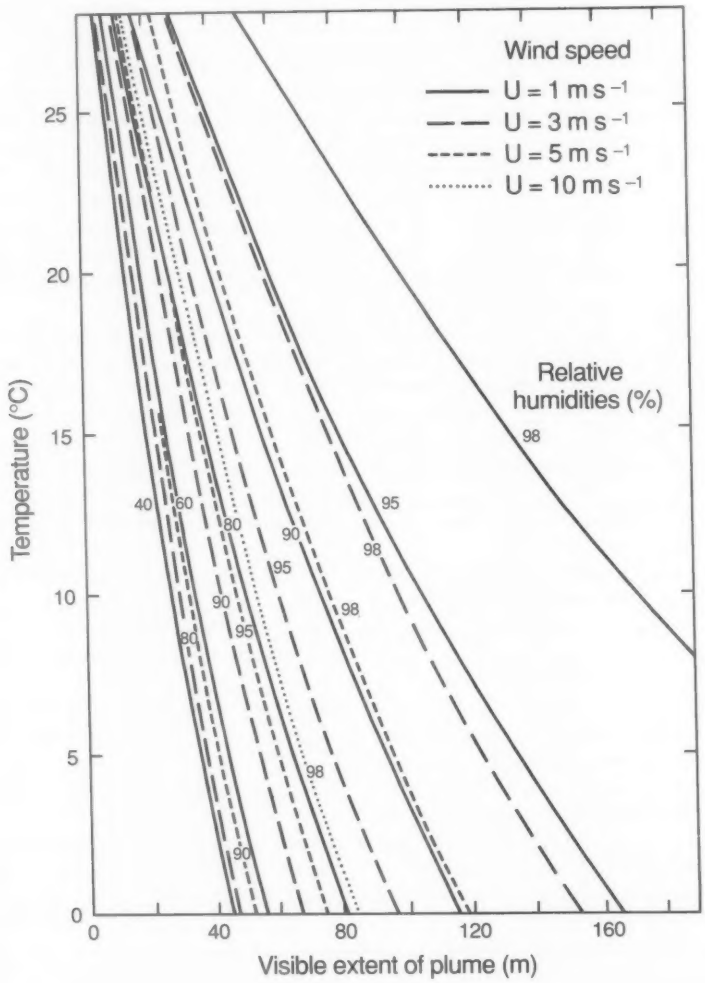

Figure 2. The maximum downwind extent of the visible plume from the stack, with different wind speeds and different ambient relative humidities and temperatures.

travelling upwards at 15 m s^{-1} and at a temperature of about 140 °C. Both these factors make the plume rise to some effective height h_e significantly greater than the stack height h_s.

The plume rise $\Delta h = h_e - h_s$ can be calculated using formulae given by Briggs (1984). Briggs states that the plume rise is given by:

$$\Delta h = \left(\frac{3F_m x}{\beta^2 U^2} + \frac{3F_b x^2}{2\beta^2 U^3}\right)^{1/3}$$

where U = wind speed in m s^{-1}, W = 15 m s^{-1}, the efflux velocity, x = the downwind distance in metres, F_m is the momentum flux, F_b is the buoyancy flux, and β is given by $(0.4 + 1.2U/W$.

However, Briggs suggests replacing β in the second term (the buoyancy term) on the right-hand side by 0.6 to be consistent with the asymptotic behaviour of buoyant plumes.

The first term in the brackets on the right-hand side of the equation is given by

$$\left(\frac{3}{4}\right)^{1/3}\left(\frac{r_o R}{(0.2 + 0.6/R)}\right)^{2/3} x^{1/3}$$

where $R = W/U$ and W = 15 m s^{-1}.

The second term is given by putting

$$F_b = g\frac{T_{stack}}{T_{air}} W r_o^2$$

where W = 15, r_o is the stack internal radius = 0.185 m, $T_{stack} = 140 + 273$, $T_{air} = 15 + 273$, $g = 9.81$.

If h_s = 23 m, then h_e is given in Fig. 3 as a function of wind speed U. The effective height h_e increases rapidly as U falls below about 3 m s^{-1}. Increasing or decreasing the stack height simply raises or lowers the effective height by the same amount.

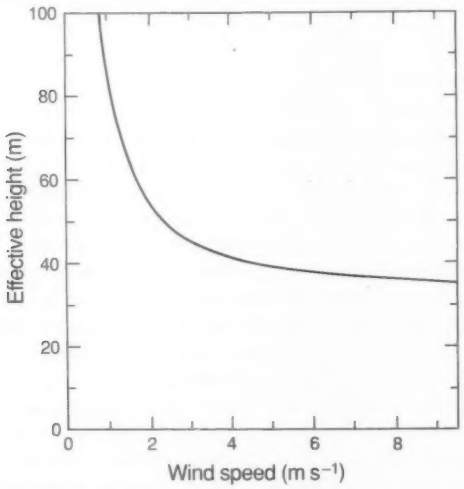

Figure 3. The effective height of the plume for a 23 m stack when the combined effects of the high temperature and the efflux velocity of the emerging plume are taken into account. Otherwise, effective height is principally a function of wind speed.

The plume rise may be ultimately halted by an elevated stable layer through which the plume cannot penetrate. However, before that, the plume may effectively level out and diffuse very much like a passive plume. It is assumed that, for modest emission rates, this occurs at 100 m downwind from the source. Since this is likely to provide an underestimate of the true plume rise, it will overestimate the ground-level concentrations to some extent.

Having so defined h_e, the plume is then assumed to act like a neutrally buoyant plume emanating from h_e. The approach of Weil (1988) is used. It is a very simple and effective method for neutral and unstable conditions. Essentially it calculates the concentration by assuming the plume elements travel along straight lines radiating out from the effective source according to the probability distribution of the turbulent velocities at the effective source. Elements are assumed to reflect off the ground or any elevated capping inversion above the source rather like light rays would off reflecting mirrors. Although this is not a perfect representation of what happens in the atmosphere, field trials indicate that the model gives reasonably satisfactory estimates of measured concentrations. Normally, out to the distance where the maximum concentration occurs, the effect of any capping inversion is not felt at ground level (except indirectly in its subtle effect on the structure of the turbulence).

The plume spreads not only vertically, of course, but horizontally as well. The acrosswind spread is particularly important in lowering the average concentration of pollutants in the plume with downwind distance. Following Briggs (1985) we assume the acrosswind distribution has a Gaussian shape:

$$C(y) = \frac{A}{\sqrt{2\pi}\sigma_y} \exp\left(-\frac{y^2}{2\sigma_y^2}\right)$$

where σ_y (the so-called 'standard deviation') is a measure of the width of the plume and is approximately given by:

$$\frac{\sigma_y}{h} = \frac{0.6X}{(1 + 2X)^{1/2}}$$

where $X = w_* x/(Uh)$, w_* is the convective velocity = $(gHh/\rho c_p T)^{1/3}$, and H is the surface sensible heat flux in W m^{-2}, h is the depth of the mixing layer.

Typical values of h, H and w_* can be ascribed to pairs of wind speed U and stability category P (see Table II). The mixing depth h strictly depends on a number of factors which are difficult to assess in any given situation without detailed meteorological data both at the time of interest and back in time along the trajectory of the air mass. Since such information is unknown in the present analysis, a rather simple approach which may introduce small errors into the results has to be used. It is believed that these errors do not significantly alter the conclusion. This belief is based on a sensitivity study by which changes in the results are obtained by changing the

Table II. A table of parameters governing the ground-level concentrations downwind of the stack. H is the heat flux in W m^{-2}, w_* is the convective velocity in m s^{-1}, h is the estimated mixing depth in metres and u_* is the friction velocity in m s^{-1}. The plume rise is given in metres as is the effective height of the source (= plume rise + stack height (23 m)).

Wind speed (average)		1–3 kn 1 m s^{-1}	4–6 kn 2.5 m s^{-1}	7–10 kn 4.25 m s^{-1}	11–16 kn 6.75 m s^{-1}	⩾17 kn ⩾9 m s^{-1}
Plume rise (m)		62	26	18	14	13
Effective h (m)		85	49	41	37	36
P	Param.					
A	H	150	300			
	w_*	1.86	2.63			
	h	1634	2368			
	u_*	0.1476	0.2928			
B	H	20	100	250		
	w_*	0.680	1.52	2.40		
	h	651	1459	2316		
	u_*	0.1176	0.2647	0.4272		
C	H	10	40	110	260	
	w_*	0.481	0.961	1.594	2.451	
	h	495	1028	1699	2618	
	u_*	0.110	0.2471	0.4056	0.6275	
D	H	0	0	0	0	0
	w_*	0	0	0	0	0
	h	217	543	923	1466	1955
	u_*	0.0869	0.2172	0.3692	0.5863	0.7821

values of h within sensible limits around the values given by our simple method.

The simple method uses the formula for the development in time of the depth of the convective mixing layer by Carson (1973):

$$\frac{dh^2}{dt} = \frac{2(1+2A)H(0,t)}{\rho c_p \gamma(t)}$$

where $H(0, t)$ is the surface sensible heat flux at $z = 0$ at time t, A is a factor to allow for the entrainment of heat from above the mixing layer and is usually given a value of 0.25, $\gamma(t)$ is the potential temperature gradient in the air above the capping inversion, and is given a default value of 0.003 °C m^{-1}. The equation can be solved for h if an analytic form for $H(0, t)$ is given. In steady meteorological conditions $H(0, t) = H_m \sin\omega t$ where H_m is the peak midday value of the heat flux, and ω is the inverse time-scale of the diurnal cycle. The maximum value of h is obtained in the afternoon, and it is this value that is used. It turns out that h depends almost entirely on H_m in a very simple way: $h = 130 H_m$. In the morning the depth of the mixing layer is likely to be less which leads to weaker turbulence and lower ground-level concentrations until the physical limits to vertical spreading imposed by the lower depth push up the concentrations to some degree at distances beyond which we are concerned.

So as to obtain the optimum estimate of h, and also to blend in with alternative estimates of h in neutral conditions, the value of $h = h_C$ given by Carson's equation is combined with $h = (u_*/4f)$ commonly used in neutral conditions:

$$h^2 = h_C^2 + (u_*/4f)^2.$$

The values of H are obtained from Smith's version of the Pasquill scheme for estimating stability. Fig. 4 shows Smith's curves which relate P, U and H. The table of parameters (Table II) also gives the convective velocity w_* and the friction velocity u_*. The convective velocity has already been defined and is used in the non-dimensional form of the downwind distance. The friction velocity, which is used in the mixing layer depth in neutral conditions, can be inferred from the 10 m wind speed and the heat flux by the following equations (which are standard equations used in micrometeorology and won't be explained properly here):

$$u_* = 0.4U / \left\{ \ln\left(\frac{(y-1)(y_o+1)}{(y+1)(y_o-1)}\right) + \right.$$

$$\left. + 0.0349(\tan^{-1} y - \tan^{-1} y_o) \right\}$$

where $y = (1 + 160/L)^{1/4}$, $y_o = (1 + 1.6/L)^{1/4}$, L is the

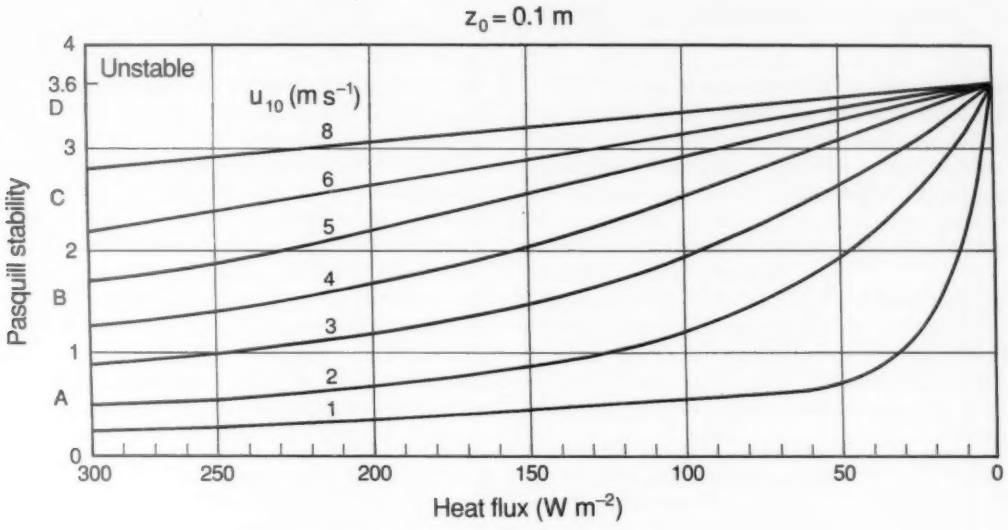

Figure 4. The revised scheme for Pasquill Stability based on heat flux and wind speed.

Monin–Obukhov length-scale $= 94\,700u_*^3/H$, and the surface roughness has implicitly been assumed to be 0.1 m. In neutral conditions $u_* = 0.087U$. To solve for u_* in convective conditions the neutral value of U_* is found, this is inserted into the expression for L to find L (for given heat flux H), y and y_o are found and inserted into the convective expression for u_*. This new value of u_* is then reinserted into the L expression and so on until a converged value of u_* is reached. To determine the ground-level concentrations, the formula provided by Weil (1988) will be used. The concentration below the plume centreline is given by:

$$C(X) = \frac{Q}{Uh^2}\,\frac{a(X)}{X}\,1.841\left\{\exp\left(-\frac{(\alpha/X-0.35)^2}{0.135}\right) + \right.$$

$$\left. + \; 0.361\exp\left(-\frac{(\alpha/X+0.4)^2}{0.461}\right)\right\}$$

where $a(X) = 0.665\,((1+2X)^{1/2}/X)$.

Q is the emission rate in g s^{-1}, $\alpha = h_s/h$, and $X = (w_*x/Uh)$.

5. Results

The equation for $C(X)$ above has been solved for $Q = 1$ g s^{-1} and for all the combinations of U and P in Table II, and for five stack heights: 10 m, 16 m, 20 m, 23 m and 30 m.

In each case the concentration distribution has the following characteristics: on the ground the concentration is zero close to the base of the stack but after some distance downwind it suddenly rises quite rapidly to its peak value, after which there is a gradually decreasing tail which persists for a long distance downwind. As an example, the results for stability $P = B$ and a wind speed of 2.5 m s^{-1} are given:

$X = 0.01 : C = 0$; $X = 0.02 : C = 0$; $X = 0.03 : C = 3.9$; $X = 0.04 : C = 27.2$; $X = 0.05 : C = 47.7$; $X = 0.06 : C = 52.1$; $X = 0.07 : C = 47.6$; $X = 0.08 : C = 40.5$, etc.

Two important conclusions can be drawn from the calculations:

(i) $C(X)$ is at a maximum with wind speeds around 2.5 m s^{-1}. For example with $P = C$ the maximum concentration varies with wind speed as follows: $U = 1 : C = 52.0$; $U = 2.5 : C = 53.1$; $U = 42.9 : C = 42.9$; $U = 6.75 : C = 29.3$;

(ii) $C(X)$ varies only very gradually with stability. C_{max} is the overall maximum concentration, regardless of where it occurs. It is given in Fig. 5 as a function of the most important parameter, h_s, the stack height. Note that decreasing h_s from 23 m to 16 m increases C_{max} from 59 to 79 μg m^{-3} with $Q = 1$ g s^{-1}. (With the proposed stack, having an emission rate of only 0.166 g s^{-1} for sulphur dioxide, the concentration increases from 10 to 13 μg m^{-2}.)

Fig. 6 shows the downwind distance x_m in metres where the maximum concentration is expected. x_m is virtually independent of wind speed U, but depends very much on stability P and h_s.

6. Maximum concentrations around the stack

Ignoring the sloping terrain in the vicinity of the stack, the concentrations of some of the pollutants emitted from the stack can be estimated.

6.1 HCl

The emission rate of HCl is given as 300 g h^{-1} or

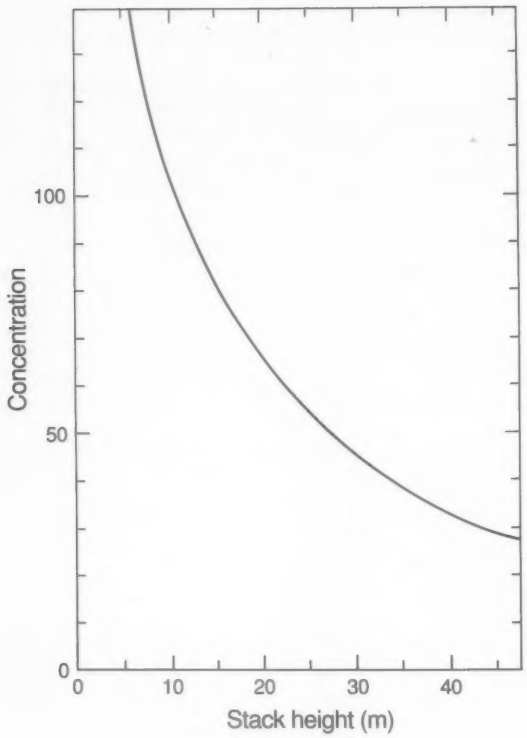

Figure 5. The 10-minute-mean peak concentration at ground level as a function of stack height for the resulting plume, but with an emission rate standardized to 1 $g\,s^{-1}$. The units of concentration are $\mu g\,m^{-3}$.

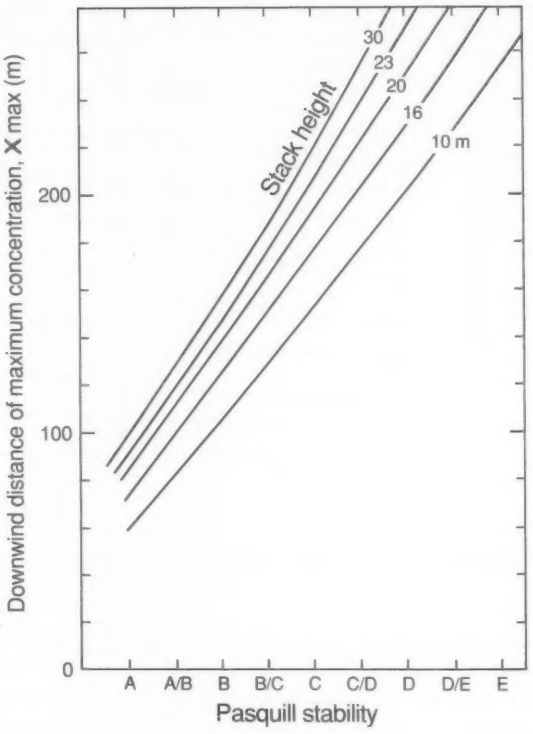

Figure 6. The distance downwind on flat terrain where the 10-minute-mean maximum concentration occurs, as a function of stack height and Pasquill Stability.

0.083 $g\,s^{-1}$. The 10-minute-average maximum concentration, as a function of h_s, in $\mu g\,m^{-3}$ is:

h_s(m) 10.0 16.0 20.0 23.0 30.0.

C_{max}: 8.7 6.6 5.5 4.9 3.8.

6.2 SO_2, NO_x, CO

The emission rate for each of these pollutants is estimated to be 600 $g\,h^{-1}$ or 0.166 $g\,s^{-1}$. The concentrations are:

h_s(m) 10.0 16.0 20.0 23.0 30.0.

C_{max}: 17.4 13.2 11.0 9.8 7.6.

6.3 The effect of the slope

It is assumed that the ground rises some 5 metres to the north-east, say; and further that a tall house exists on the highest ground and is some 8–10 metres tall, so that its upper rooms may be some 14 metres above the base of the stack.

The slope of the ground will only be important in the relatively few cases of daytime stable conditions when, due to the increase of air temperature with height, air motions tend to be much more horizontal than in neutral or unstable conditions when the air readily follows the contours of the underlying terrain.

Although stable conditions can and do occur at any time of the day if the meteorological conditions are right, they most frequently occur soon after dawn and in the late afternoon an hour or so before sunset. They tend to develop whenever the winds are light and the skies are cloud-free. To avoid the great majority of these cases, it would be prudent to recommend, in this assumed scenario, that the stack should not be operated with very light winds after, or before, a cold night, with a south-westerly drift moving the air up the slope towards the tall house to the north-east, until at the earliest 9 a.m., or until the latest 4 p.m. Under these stable conditions the upper rooms of the house would otherwise be subject to emissions from a stack that is effectively 14 metres lower. Calculations show that for a 23-metre stack this apparent reduction doubles the maximum concentration likely to be experienced, even though the centreline of the plume will still easily clear the top of the house. In reality the proposed restriction will impose very little extra constraint on the stack's operation since firing would not normally take place at either end of the working day.

More precise criteria could be proposed, and a simple warning scheme arranged with the Meteorological Office at the nearest forecasting office.

7. Frequency data of the meteorological parameters

No meteorological observing station exists in Midville itself, and the nearest fully operational station is at Elmdon. Although some distance away, it is considered that the statistics of the relevant parameters are likely to be very similar. Between 08 and 18 UTC the Pasquill Stability Categories occur with the percentage frequencies given in Tables III and IV. All the stable cases (E, F and G) occur either at 08, 16, 17 or 18 UTC. The highest percentage frequency is seen to be in the neutral D category, and over 92% of hours at Elmdon lie within C–D, i.e. in neutral or slightly unstable conditions. The more unstable conditions tend to occur around midday when the incoming solar radiation is at its highest.

Fig. 7 shows the wind rose for Elmdon, which is less than 20 km to the north-west, as well as for Brize Norton (further to the south) and Wyton (more than 100 km to the east). A very similar wind rose to that for Elmdon should apply to the stack. South-west winds are seen to be considerably more frequent than other winds. The sector from south to west contains 75% more winds than the average in the north-east.

Between 08 and 18 UTC, the wind speed classes have the percentage frequencies as set out in Table V. As can be seen, very light winds below 2 m s^{-1} occur in about 5–6% of all hours, but many of these would be at night when the incinerator would not be operating.

Table III. Percentage frequencies of Pasquill stability categories at Birmingham Airport (Elmdon), Brize Norton and Wyton during daytime (08–17 UTC)

P	A	B	C	D	E	F	G
Elmdon	0.38	4.13	24.72	67.39	2.52	0.57	0.28
Brize Norton	0.32	3.96	22.76	69.73	2.17	0.67	0.28
Wyton	0.30	3.81	22.33	67.43	2.49	0.50	0.14

Table IV. Pasquill Stability Category frequencies by hour at Elmdon 1980–89

Hour (UTC)	Pasquill Stability Category A	B	C	D (day)	D (night)	E	F	G	Total
0	0	0	0	0	1068	1523	639	422	3652
1	0	0	0	0	1051	1518	637	446	3652
2	0	0	0	0	1066	1490	619	477	3652
3	0	0	0	0	1078	1492	583	499	3652
4	0	0	0	400	1003	1329	530	390	3652
5	0	0	0	1160	837	1045	354	256	3652
6	0	0	21	1739	720	781	229	162	3652
7	0	2	297	2050	510	549	151	93	3652
8	0	53	603	2373	261	259	51	52	3652
9	4	147	927	2574	0	0	0	0	3652
10	20	211	1227	2194	0	0	0	0	3652
11	33	258	1348	2012	0	0	0	0	3651
12	36	268	1315	2033	0	0	0	0	3652
13	29	233	1207	2183	0	0	0	0	3652
14	14	189	975	2473	0	0	0	0	3651
15	3	111	726	2812	0	0	0	0	3652
16	0	37	490	2732	187	165	31	10	3652
17	0	2	209	2287	489	496	126	42	3651
18	0	0	16	1883	689	754	222	87	3651
19	0	0	0	1300	865	1012	325	150	3652
20	0	0	0	620	1007	1325	493	207	3652
21	0	0	0	0	1124	1630	634	263	3651
22	0	0	0	0	1093	1613	638	307	3651
23	0	0	0	0	1081	1564	637	369	3651
Total	139	1511	9361	32825	14129	18545	6899	4232	87641

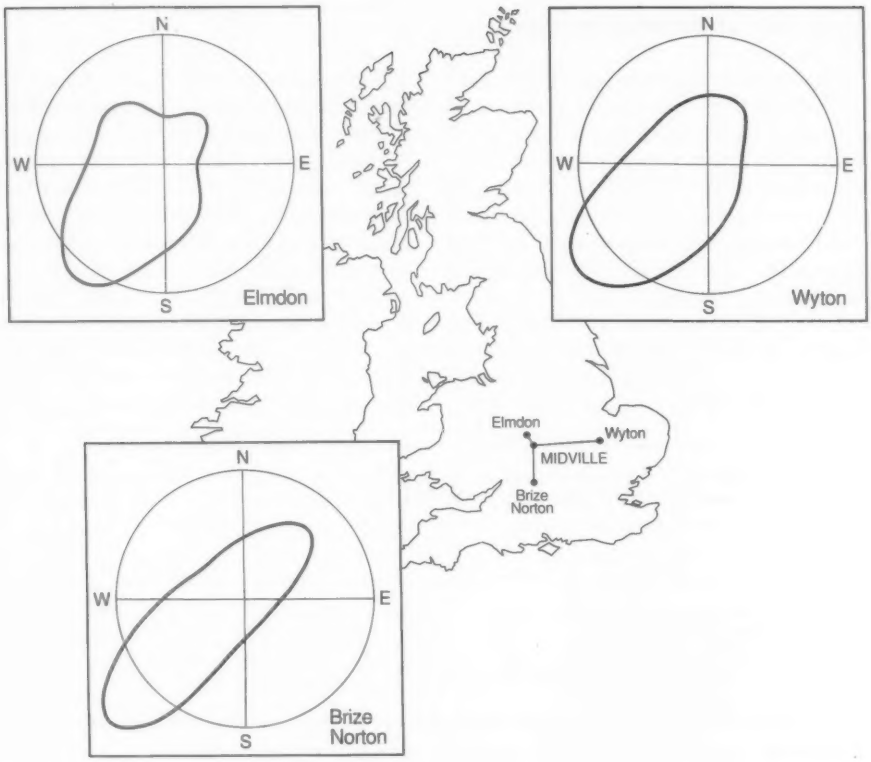

Figure 7. The wind rose at Elmdon (Birmingham Airport) shows the predominance of south-westerly winds, the circle delineating the 14% frequencies. The wind roses at Wyton and at Brize Norton have the same characteristic.

Table V. Wind speed percentage frequencies at Elmdon, Brize Norton and Wyton between 08 and 18 UTC. The *U* values are average values in the wind speed ranges. The frequencies are similar at the three stations.

Wind speed (kn)	*U* ($m\ s^{-1}$)	Percentage frequencies Elmdon	Brize Norton	Wyton
Calm	0	5	3	2
1–3	1	14	20	11
4–6	2.5	25	21	20
7–10	4.25	32	29	33
11–16	6.75	20	22	27
17–98	9	4	5	7

Conditions of high humidity (leading to long, visible plumes extending 100 metres or so) are very unusual during summer daylight hours; a relative humidity greater than 95% during the day occurs less than 4% of the time between May and the end of August.

In winter, however, this increases to around 30% at 9 a.m. between November and February, and 10% at 3 p.m. The required cold temperatures would also be experienced only in winter for such long plumes.

References

Briggs, G.A., 1984: Plume rise and buoyancy effects. *In* Randerson, D. (ed.); Atmospheric science and power. DOE/TIC 27601, US Department of Energy.

—, 1985: Analytical parametrizations of diffusion: the convective boundary layer. *J Clim Appl Meteorol*, **24**, 1167–1186.

Carson, D.J., 1973: The development of a dry inversion-capped convectively unstable boundary layer. *Q J R Meteorol Soc*, **99**, 450–467.

Weil, J.C., 1988: Dispersion in the convective boundary layer. *In* Venkatram, A. and Wyngaard, J.C. (eds); Lectures on air pollution modeling. Boston, American Meteorological Society.

551.583.1

The role of observations in climate prediction and research*

D.J. Carson
Meteorological Office, Bracknell

Summary

The main uses of climate data are listed. Some comments are made on the data requirements for climate modelling, detection and diagnostic studies. The discussion concentrates mainly on the data needed to provide boundary conditions, initialization and validation for climate models.

1. Introduction

Many uncertainties surround our understanding of, and ability to model, the climate system. These, and other technical limitations, make prediction of the nature, magnitude and timing of climate change, particularly at scales smaller than global, unreliable at present. Increasing concern over the need to detect, understand and predict global and regional environmental changes has highlighted the need to establish high-quality observational data sets relating to the earth's atmosphere, oceans, cryosphere and land-surface. The basic climate record needs to be better established from geological times up to the present and decisions must be taken now to ensure more comprehensive global data coverage of the climate system in future.

A prerequisite to designing and implementing a Global Climate Observing System (GCOS) is to identify the principal uses and users of the data to be collected in order to justify such a costly, long-term, internationally collaborative operation.

The major requirements for data in support of climate prediction and research, the latter to be interpreted in its widest sense, are for:

(a) monitoring the climate and its variability at global and regional scales, thereby enabling quantification of natural climatic fluctuations on a range of temporal and spatial scales and the detection of climate change,

(b) attribution of climate change to particular causes, as in the search for a fingerprint which will enable detection and attribution of climate change due to an enhanced greenhouse effect resulting from man-made emissions of greenhouse gases,

(c) detection (and attribution) of the environmental impacts of climate change,

(d) diagnostic studies to elucidate the behaviour of the climate system and its component parts, namely, atmosphere, oceans, land surface, cryosphere, etc. including studies of the mechanisms of natural climatic variability,

(e) development and testing of hypotheses relating to local and global climate variations and to the degree of predictability of climatic phenomena,

(f) process studies. Special data are needed in support of detailed research studies of a wide variety of complex dynamical, physical, chemical and biological processes which help govern the state and evolution of the climate system. Such specialized data sets are likely to need to be highly resolved in time and space and therefore gathered for a limited period over a restricted area of the globe. High-priority process studies include cloud–climate and air–sea interactions,

(g) providing boundary conditions for climate models. These include surface properties such as albedo, roughness length, vegetation index, soil physical parameters, etc. Some such data are also needed to identify changes in relevant surface properties, e.g. due to deforestation (see also (c) above),

(h) initialization of climate model integrations, especially of the oceanic and cryospheric components, and also some of the land-surface hydrological characteristics such as the 'soil moisture content',

(i) validation of climate models. A very wide range of data, including palaeoclimatic data, are needed to assess the performance of the models being used for climate simulation and prediction. Model behaviour is compared with that of the 'observed' climate, often leading to further development and improvement of the models, and

(j) data-assimilation techniques for climate model development. Aspects of the climate models can be improved through the use of climate observations in sophisticated four-dimensional data-assimilation schemes, such as those used with state-of-the-art operational weather forecasting models.

Although model and observational studies are becoming increasingly interdependent, it is convenient for the points to be focused on primarily in this article to consider the requirements (a)–(f) above as being, in the

* Background paper prepared for the World Climate Research Programme *ad hoc* Workshop on the Planning of the Global Climate Observing System, 14–15 January 1991, Winchester, England.

main, model-independent, whereas (g)–(j) are directly related to the development and use of climate-simulation and prediction models. A few comments on the data requirements for climate monitoring and diagnostic studies are given in section 2. Section 3 concentrates on the observational needs of climate-simulation and climate-prediction models, i.e. items (g)–(j) above.

It is worth stressing that the above needs and uses encompass a variety of types of data, for example :

'Stand-alone' instrumental data, including data from both *in situ* and remote-sensing (in particular satellite-borne) instruments. Examples of the former are surface and upper-air temperatures, rainfall, etc. The latter category also includes surface and upper-air temperatures, and cloud cover, etc.

'Blended' data, i.e. a data set produced from more than one data source; e.g. sea surface temperatures derived from both satellite- and ship-borne sensors.

(Climate studies are by their very nature global in character and this necessitates extensive use of space observations to provide the necessary coverage and continuity. Space observations are, however, in many respects difficult to interpret and special blending techniques are required in order for them to provide reliable information for climate research. In particular, they need to be combined with *in situ* observations to resolve ambiguities in their interpretation, to provide higher precision, and to enable estimates of fields of derived quantities, such as surface heat and moisture fluxes.)

Data assimilated by operational weather forecasting models. This is a powerful technique for the optimal combination of space-based and *in situ* observations. It provides 'complete' global data sets which are internally, dynamically and physically consistent, e.g. 3-dimensional, global wind fields. However, biases may be introduced by changes to the models used.

'Derived' data, i.e. data calculated from other directly measured or assimilated data, e.g. derived surface fluxes of heat, moisture and momentum. Information on land-surface characteristics, such as albedo and surface roughness, are usually 'derived' from a 'blend' of a variety of data types.

2. Data requirements for monitoring, detection and diagnostic studies

Studies of climatic processes often require short-lived specialized regional-scale data sets and associated field programmes. Studies of climate variability, change and predictability demand long-time-scale (decades to centuries or more) data sets which are homogeneous in time, i.e. without bias or with a constant bias. Studies of global environmental change (including climate change) clearly require global data sets, and regional variability, change and predictability are being studied increasingly in the context of the corresponding global-scale characteristics. The climate data sets to be assembled must reflect these diverse needs.

The 'operational' and research needs will also often lead to a hierarchy of data sets for a given variable, e.g. a real-time data set (used for operational weather forecasting, and for monthly and seasonal predictions), a delayed-mode data set (containing more data than the real-time one, and useful for preliminary monitoring and research studies), and a slow-mode data set (containing all available data with instrumental corrections, e.g. historical *in situ* sea surface temperature data sets).

Beside the routine production of analyses for climate research using data-assimilation techniques, it is essential to continue to process selected *in situ* and remotely sensed observations independently from the integrated data-assimilation systems. This is because information is needed on the atmosphere and oceans (for example, ocean and land surface temperature analyses) which are free from the biases that arise from the inclusion of (changing) modelling assumptions. For selected variables, long time-series of observations need to continue to be carefully processed to produce analyses which are as free as possible from the influence of changes to the observing or processing techniques introduced over the period. 'Pure-data' archives are necessary for this purpose. A particularly important example for validating climate models is the need for a reliable, homogeneous archive of atmospheric data from radiosondes.

For monitoring climate, quantifying climate variability and detecting climate change, a long historical perspective is needed, in contrast to the normal data requirements in operational weather forecasting. In this context, it is important to realize that many historic data are not yet in a form for use on computers. Indeed many of the data needed for climate purposes are not expected to be processed through data-assimilation schemes in the medium-term future. Criteria for the collection and assembly of data sets for climate monitoring include :

Data are required for different parts of the climate system, particularly for atmosphere and oceans.

There is a need to establish reliable homogeneous quasi-global historic 'base-line' data sets.

Current data need to be homogeneous with historic data; this is a difficult task and specialized techniques need to be developed to achieve the necessary high levels of homogeneity.

Satellite data need to be blended with more-conventional data.

Near real-time data are required to monitor short-period weather variability on time-scales ranging from a day to a month. Few daily data are available on the global scale and this prevents worldwide monitoring of extreme events such as frosts.

In the context of short-period weather variability it is worth noting the additional data needs for long-range (monthly–seasonal) forecasting. This activity requires daily, real-time global data sets with special requirements for particular regions (e.g. high-resolution climate data for the United Kingdom are needed for the long-range forecasting activities within the Meteorological Office). Also, long-range forecasting based on statistical methods needs long, homogeneous historical data sets.

Some suggested data sets for climate monitoring are listed in Table I. Many of the qualifying column entries in this table are somewhat tentative.

Diagnostic studies of data to explore climate mechanisms and processes, especially studies of low-frequency weather variability, have some additional and different requirements. The overriding need is for 3-dimensional, high-resolution, physically and dynamically self-consistent global data sets. This is generally only feasible by use of data assimilation allied to a global model. Data are needed at least twice daily (preferably 6-hourly) to avoid biases that can be introduced by diurnal effects. Homogeneity is another important requirement, but cannot always be achieved. Many of the data sets to be analysed are of derived physical and dynamical properties of the atmosphere and, where possible, the oceans, e.g. diabatic heating rates, eddy fluxes, ageostrophic quantities, etc.

3. Data needs for climate modelling and prediction

Some comments are offered on the following aspects of the data requirements in connection with the development and use of global numerical models for studying and predicting climate and climate change:

Boundary conditions.
Initialization.
Validation.
Data-assimilation techniques for model development.

3.1 Data for model boundary conditions

This encompasses a wide range of data which are prescribed in order to run climate models in various configurations (namely, atmosphere-only, ocean-only, coupled atmosphere–ocean). They may be held constant or updated prescriptively throughout a model integration, but they are not determined prognostically or diagnostically within the model itself. A range of boundary conditions is needed for application at the land-surface or air–sea interface, in the upper reaches of the atmosphere, throughout the atmosphere, oceans and soils, and at the lower ocean boundary.

The need to prescribe such boundary conditions depends to a very large extent on the state of development of the model being used, the configuration it is being used in, and what it is being used for. As models of the full climate system develop, and as they are used increasingly for making predictions of transient global and regional climate change, then correspondingly more degrees of freedom will be given to such models and the requirements for boundary conditions will evolve in response. Some quantities acknowledged at present as boundary conditions will become full prognostic variables in the models, whilst new boundary conditions will be needed for new and more complex representations of the sub-grid-scale processes (i.e. new parametrizations will require new boundary conditions).

Examples of important boundary conditions requiring better global data sets are :

Atmosphere-only models:
Sea surface temperatures (SSTs).
Sea ice extent, concentration, thickness.
Ozone distribution.
Land-surface characteristics (albedo, surface roughness length, vegetation type, etc.).
Land ice extent and thickness.
Orographic height (and sub-grid-scale variance).

Ocean-only models:

Aside from ocean bottom topography, the prime requirement here is for data to provide the surface forcing needed for ocean model integrations, namely:

Surface stress fields.
Wind mixing.
Heat fluxes (incoming solar and long-wave radiation, sensible and latent heat fluxes) and freshwater (precipitation less evaporation) fluxes.
River runoff.

Two basic approaches may be made to provide the appropriate forcing for the model, though in practice a combination of the two is frequently used.

The fluxes may be specified directly, in which case it is necessary to use a 'flux-correction' technique whereby the net heat flux (Q_o) is modified by a feedback term which helps to constrain the predicted sea surface temperature (T_p) in the model to the observed field (T_o) depending on the size of the feedback parameter (k), i.e. the applied heat flux (Q) is given by:

$$Q = Q_o + k(T_o - T_p).$$

A similar approach may be used for the freshwater flux, which is then constrained to the observed salinity field.

Alternatively, the basic meteorological parameters necessary to drive the turbulent fluxes can be specified and the fluxes derived via appropriate bulk formulae as the integration proceeds and with reference to the modelled SST (or ice surface temperature) where appropriate. In this case the data sets required are:

Surface wind field.
Wind mixing.
Surface air temperature.
Surface air humidity.
Surface pressure.

Table I. Data for climate monitoring (tentative)

Parameter	Data sources		Data types		Priority	Accuracy or precision	Desirable accuracy of long-term changes	Spatial resolution		Time resolution
	In situ	Remote	Pure	Assimil-ated	XXX suggests highest			Horizontal	Vertical	
SST	✓	✓	✓	✓	XXX	0.2 °C local or region 0.1 °C global	≤0.1 °C	100 km		2 weeks
Sub-surface ocean temperature	✓		✓	?	XX	0.1 °C	0.05 °C	500 km?	20 m above thermocline, 0.2 km below	Monthly
Marine surface air temperature	✓		✓	✓	XX	0.2 °C local and region 0.1 °C global	≤0.1 °C	500 km?		Monthly
Land surface air temperature	✓		✓	✓	XXX	0.2 °C local and region 0.1 °C global	≤0.1 °C	500 km		Monthly and daily
Atmospheric temperature	✓	✓	✓	✓	XXX	0.5 °C local 0.1 °C global	≤0.2 °C	500 km	1–2 km	Monthly
Humidity	✓	✓	✓	✓	XX	5–7% specific humidity	1% specific humidity	500 km	2–3 km	Monthly
Surface wind	✓	✓	✓	✓	XXX	1 m s^{-1}	≤1 m s^{-1}	500 km		Monthly
Winds aloft	✓	✓	✓	✓	XX	1 m s^{-1}	≤1 m s^{-1}	500 km	1–2 km	Monthly
Surface pressure	✓		✓	✓	XXX	1 mb	≤1 mb	500 km		Daily
Atmospheric geopotential heights	✓	✓	✓	✓	XXX	10 m	≤10 m	500 km	1 km	Daily
Precipitation over land	✓	✓	✓	?	XXX	10% daily 5% monthly	≤2%	Variable		Monthly and daily
Precipitation over ocean	If possible	✓	✓	?	XX	20%	≤5%	500 km		5 days?

Cloudiness variables	✓	✓	✓		XXX	Complex (10% of total amount)	Complex (≤ 5% of total amount)	250 km	1 km	Monthly or less
Sea ice extent	✓	✓	✓	?	XXX	5% open water	1% open water	100 km?		Monthly
Sea ice thickness	✓	?	✓	?	XXX	10% or 0.5 m?	2% or 0.1 m?	100 km		Monthly
Snow extent	✓	✓	✓	?	XXX	3%	1%	100 km?		3 days
Snow depth	✓	?	✓	?	X	20%?	< 5%?	100 km?		3 days
Salinity	✓	?	✓	?	XX	2%	1%	250 km	0.2 km	Monthly
Near surface ocean currents	✓	✓	✓	✓	XXX	2 cm s^{-1}	5%	20 km in major currents	0.2 km	Monthly
Sea surface height	✓	✓	✓	✓	XXX	5 cm	2 cm	200 km?		Monthly or less
Soil moisture	Few	?	?	?	XXX	10% of field capacity	2% of field capacity	100 km?	10 cm	Monthly and 5-daily
Vegetation		✓	✓		XX	10% of total biomass	5%? of total biomass	100 km		Monthly
Planetary radiation budget components		✓	✓	?	XXX	10 W m^{-2}	≤ 0.5 W m^{-2}	250 km?		Monthly
Solar 'constant'		✓	✓		XXX	0.05%	0.01% (≈ 0.1 W m^{-2})			Monthly
Atmospheric CO_2 concentration	✓		✓		XXX	0.5 ppm	0.5 ppm	Global		1 year
Atmospheric diagnostics	✓	✓		✓	XXX	5%	1%	500 km	1–2 km	Daily and 6-hourly

Incoming solar and long-wave radiation/cloudiness.

Coupled atmosphere–ocean general circulation models (AOGCMs):

Particular boundary data sets required here are:
Ozone distributions.
Land-surface characteristics, including land ice extent and thickness.
Topographic data for both land and oceans.

3.2 Data for model initialization

These are data needed to set the initial values of variables which will then be updated, usually prognostically, within the model itself. It is often not understood that climate modelling and climate prediction are not initial-value problems in the same way that short- to long-range forecasting are initial-value problems — at least as far as initializing the atmosphere is concerned. Initialization of the atmosphere is not a critical factor in climate modelling or prediction; it is quite acceptable to use model-compatible data from a single time from a previous climate model run or a numerical weather prediction analysis, and quite unnecessary and of no additional value to demand real-time global analyses.

In the current state of development of climate models, it may be more critical to initialize aspects of the land-surface prognostic variables, if not starting from a previously derived model data set. In particular, there is modelling evidence of long-lasting effects of the initial values used for some of the land-surface hydrological characteristics. Snow cover, soil moisture content and soil temperatures are examples of variables which may need to be initialized by 'spinning up' the model through at least a seasonal cycle.

The main current (and probably future) requirements for initializing climate models concern the oceans, whether in ocean-only models or coupled AOGCMs. Global fields of profiles of temperature, salinity and currents are required to provide a realistic initialization of ocean models. Currently the Levitus global temperature and salinity data set is used and the currents generated as the model runs. Repeated insertion of Levitus data may be useful and valid for high-resolution ocean models in this context (such as that used in NERC's FRAM project). Long (centuries or more), costly, computer integrations are necessary for the models to come into equilibrium with any specified forcing. Note that the final state may depart significantly from the 'observed' state.

Aspects of the cryosphere also require careful initialization in climate models. In particular, as a minimum, sea ice extent needs to be initialized. There is also need for sea ice concentrations and thicknesses, although the latter are particularly difficult to achieve.

In coupled AOGCMs a major problem is to bring the component systems into mutual adjustment with one another. The length of model integration necessary to achieve sufficient adjustment (and estimate flux corrections) for a given purpose may vary from decades to millenia. The initial data requirements for AOGCMs are as above. There is no doubt that initialization of the ocean component of the climate system presents by far the greatest challenge in this area of climate modelling and prediction. Note that careful specification of the 'observed' state is particularly necessary for TOGA-related predictions and hindcasts (e.g. the prediction of ENSO events).

3.3 Data for model validation

The IPCC WG1 Report identifies three categories of data needed for climate model validation:

(a) variables important for description of the atmospheric and oceanic circulation,
e.g. atmosphere: mean-sea-level pressure; wind and temperature profiles; variability as indicated by eddy kinetic energy, and
ocean: surface dynamic height (not often calculated in models); temperature, salinity and current structure; distribution of tracers; eddy statistics,
(b) variables critical in defining climate change,
e.g. atmosphere: surface air temperature; precipitation; soil moisture; monthly means plus interannual and daily variability, and
ocean: SST; ocean mixed-layer depth, and
(c) variables important for climate feedbacks,
e.g. snow cover; sea ice; clouds and their radiative effects.

Note that the above categories (a)–(c) are not mutually exclusive and many types of observations fit equally well into more than one.

Validation of selected regional aspects is also of relevance, e.g. occurrence of ENSO events in coupled models, and monsoon phenomena.

There are again particular considerations when verifying ocean models. On the seasonal time-scale, data are needed to validate simulations of the upper ocean mixed layer. Data on the spread of transient tracers provide valuable verification of decadal time-scale changes in the ocean. On the time-scale of a century or more data on deep ocean temperature and salinity structures, as well as of other tracers, will be of value.

Particular requirements for validating results from coupled AOGCMs include data on surface fluxes, SST and sea ice (extent, concentration and thickness).

3.4 Additional comments on the needs for boundary conditions, initialization and validation of climate models

Table II lists some of the recognized data requirements for initializing, validating and providing boundary conditions for climate models.

Data are needed with a range of temporal resolutions: monthly means and variances, both on a climatological basis and for individual months; daily data are explicitly required in some cases as are data on the diurnal cycle of some quantities.

Table II. Data required to provide initialization, validation and boundary conditions for climate models (tentative)

	Boundary	Initialization	Validation
Atmosphere			
T, q, V (surf & u/a)	★ (surf)		•
Cloudiness	★		•
Radiative fluxes (surface, vertical profiles & TOA)	★		•
Precipitation	★		•
Surface fluxes	★		•
Ozone	•		•
Land surface			
Albedo	•		•
Snow depth		•	•
Vegetation	•	(•)	•
Runoff	•		•
Soil moisture		•	•
Surface temperature		•	•
Topography	•		
Roughness	•		
Sea ice			
Extent/concentration	•	•	•
Thickness	•	•	•
Roughness	•		
Ocean			
Dynamic height		(•)	•
Surface *T, S, V*	• (SST)	•	•
T, S, V structure		•	•
Mixed-layer depth		•	•
Wave characteristics (height etc.)			•
Tracers		•	•
Water type (plankton, CO_2, etc.)	•		

Size of dots signifies probable importance.
★ signifies over ocean only.

Future model assessments would benefit particularly from improved data sets on:

Precipitation and evaporation rates over the oceans.

Evapotranspiration, soil moisture and snow depth over land.

Clouds.

Ocean properties (temperature, salinity, currents, etc.).

Sea ice.

With regard to the potential of climate data sets produced by means of sophisticated data-assimilation techniques there is a need for climate modellers to explore more thoroughly how 'operational' archives can be utilized more comprehensively for model validation. There is still considerable capital to be extracted from existing data sets and scope for carefully considered reanalyses of data from the recent past, using a fixed model.

There is increasing need to ensure that data are made available in machinable form, compatible with what models require. In that context, more-uniform practices need to be adopted in the retention of the model data which are needed increasingly for model intercomparison studies, e.g. snow-cover frequency and depth, extremes and means of daily near-surface temperature.

3.5 Data for assimilation techniques for development of climate models

There are insufficient observations at any one time to determine the state of the atmosphere (even less for the oceans). Therefore we need to invoke any additional information we have, and this is available indirectly as the knowledge of the behaviour and structure of the atmosphere and, to a lesser extent, of the oceans, which we have encapsulated in the formulations of our operational weather forecasting and climate models. In particular, knowledge of evolution with time is embodied in operational forecasting systems and this enables the use of data distributed in time. Such models also provide a dynamically and physically consistent means of representing the atmosphere and oceans, and of deriving fluxes and other diagnostic quantities.

Assimilation is the process of finding the model representation which is most consistent with the available observations. Given observations distributed in time and space, and a forecast model, we can perform a 4-dimensional data assimilation. This is normally done by adding observations as the model is integrated forward in time. The current model-state summarizes in an organized way the information from earlier observations and, given new observations, the model state is modified to be consistent with these and the earlier information.

It should be emphasized that at any given time the model state usually contains more information than can be extracted solely from the currently available observations. However, only variables which are well represented in the weather forecasting model can be assimilated sensibly in this way. There is considerable need and scope therefore for developing data assimilation techniques to process new types of observations within the framework of model assimilation in order to calculate the misfit between observed (or subsequently derived) properties and those produced (or diagnosed) from climate model integrations. Such observational and model comparisons can be used to validate and improve the representation of the physical processes in models and, conceivably, when such parametrizations have been demonstrated to represent an observed property adequately, then the model can be developed into a full assimilation using inverse methodology.

Acknowledgements

The above notes on the role of observations in climate prediction and research were compiled following discussions with several colleagues in the Meteorological Office. I am indebted in particular to H. Cattle, C.K. Folland, A.C. Lorenc, J.F.B. Mitchell, D.E. Parker and P.R. Rowntree.

Awards

L.G. Groves Memorial Prizes and Awards for 1989

At a joint ceremony at RAF Odiham on 10 December 1990 The Chief of Air Staff, Air Chief Marshal Sir Peter Harding, GCB, ADC, D.Sc., F.R.Ae.S., CBIM, presented the Wilkinson Battle of Britain Memorial Sword to the Support Helicopter Force and the L.G. Groves Prizes and Awards to the prize-winners. Air Vice-Marshal D.O. Crwys-Williams, RAF, Director General of Personnel Services, Air Officer Commanding No.1 Group, read the citations and announced the prize-winners.

Meteorology Prize — A.C. Lorenc

The citation for this award was:

'Mr Lorenc is one of the world's leading experts on research into effective methods of processing meteorological observations automatically to provide initial conditions for numerical weather forecasts. A hallmark of his work is its sound theoretical basis and its clear practical applicability.

Recently he showed that quality-control procedures could be built upon well-found statistical principles, and he demonstrated that automatic techniques can supplant time-consuming human scrutiny of data for errors.

Another of his innovations is the scheme currently used to provide operational analyses. One of its features is the ability to assimilate asynoptic observations (such as aircraft data) at the actual time that the measurements were made rather than (as was previously done) at the nearest 6-hour time slot; such a procedure makes better use of the data especially in rapidly developing synoptic situations. Its operational implementation in late 1988 has lead to improvements in the accuracy of wind forecasts for aviation.

More recently his attention has turned to the effective use of remotely sensed data. He is Principal Investigator for the American Earth Observation Satellite and for the European ERS-1 satellite. His advocacy of the use of numerical model forecasts, rather than climatology, as a first guess for satellite-derived temperatures has led to improved forecasts, and has strongly influenced US meteorologists to adopt a similar approach.'

Meteorological Observation Award — W.D.N. Jackson

The citation for this award was:

'Mr Jackson has been at the Meteorological Research Flight for 3½ years. During this time he has been in charge of the team of about 20 people responsible for the aircraft instrumentation and the airborne and ground-based computer systems used to analyse the resulting data. He has caused significant improvements and advancements in all these areas and during 1990 a new display and analysis system was completed. Large parts of these systems were designed and implemented by Mr Jackson himself. The end result is much better aircraft utilization due to both the new real-time displays of data on the aircraft and the ability to analyse flight data in detail overnight so as to identify problems and issues prior to subsequent flights. In addition to these technical advances Mr Jackson has created an atmosphere in which the staff recognize the importance of aircraft availability and have a framework within which to strive to maximize it. He has made a most significant contribution to the observing programme of the Meteorological Research Flight.'

Other prizewinners

The Air Safety Prize was presented to Flt. Lt. R.L. Foulkes B.Sc., RAF, but the Ground Safety Award was not presented as the prize-winner, Sqn. Ldr. M.A. Calame, RAF, was unable to attend.

Correction

Meteorological Magazine, April 1991, p. 73, Review of *Global Air Pollution.*

The specific reference to Professor Scorer's book was accidentally transposed to the second paragraph, but should have been included at the end of the first paragraph, as an alternative book to the one under review. Apologies are offered for any implied misrepresentation.

Satellite photographs — 2 February 1991 at 1533 UTC

The NOAA-11 pictures exhibit features which have come to be recognized as hallmarks of the onset of explosive cyclogenesis.

The images display several prominent features as highlighted on the schematic diagram in Fig. 1:

(a) Cloudy band, F, which is symptomatic of a warm conveyor belt flow associated with a well-established cold front.

(b) The 'cloud head' or 'baroclinic leaf', C, which is particularly striking. It is interpreted as a region of strong slantwise ascent occurring rearwards of a newly developing front RR. The corresponding infra-red image reveals a transition from warm cloud tops at the eastern edge of this cloud shield to coldest cloud tops near its sharply defined western boundary — a feature typical of slantwise ascending motion.

(c) A narrow cloud-free region separates cloud masses C and F — this is particularly prominent on infra-red imagery. Such 'dry intrusions' or 'dry wedges' (see Monk and Bader*) are often a feature of rapidly deepening depressions.

Further to the west, streets of convective cloud, P, stream eastwards around an upper trough, the accompanying cold advection reinforcing the thermal gradient along the new frontal zone. Lines of convective cloud can be seen undercutting the overhang of cirrostratus.

The southern, cyclonically curved, tail of the cloud head consists only of low cloud, at the leading edge of which is a well-marked narrow 'rope cloud' (RR). This probably represents line convection at the surface cold front which has been overridden by the intrusion of dry air aloft.

The transverse striations in the cloud head have been observed previously, notably in the Great Storm of October 1987 (see Shutts†), but are not fully understood. The latitudinal banding became less pronounced in later satellite passes, obscured by thickening cirrus layers generated by continued slantwise ascent.

The developing low, L, was estimated to have been centred near the northern end of the rope cloud, with a central pressure of about 990 mb. The midday operational analysis of the fine-mesh model had identified only an open wave of about 1000 mb, but 24 hours later the low had deepened to below 935 mb as it crossed Iceland, causing extensive structural damage. Many Icelandic stations observed hurricane force winds: Vestmannaeyjar on the south coast reported a mean wind of 103 kn at 1200 UTC on 3 February.

Although the numerical weather prediction guidance based on data at 1200 UTC on 2 February failed to capture the intense degree of cyclogenesis, the imagery was used as a basis for adjusting later model analyses to

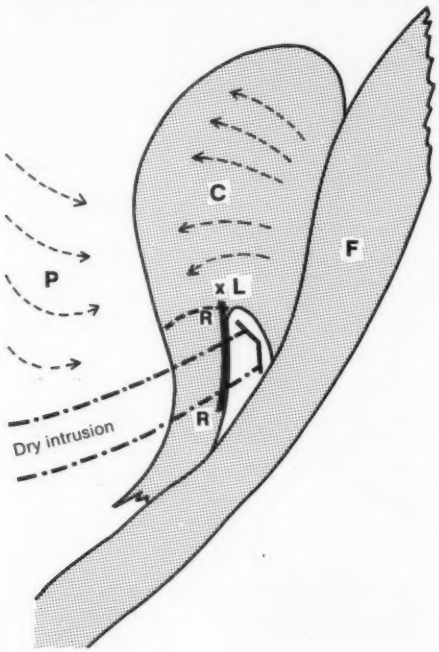

Figure 1. Schematic diagram of the features described in the text.

* Monk, G.A. and Bader, M.J.; Satellite images showing the development of the storm of 15–16 October 1987. *Weather*, **43**, 1988, 130–135.

† Shutts, G.J.; Dynamical aspects of the October storm 1987: A study of a successful fine-mesh simulation. *Q J R Meteorol Soc*, **116**, 1990, 1315–1347.

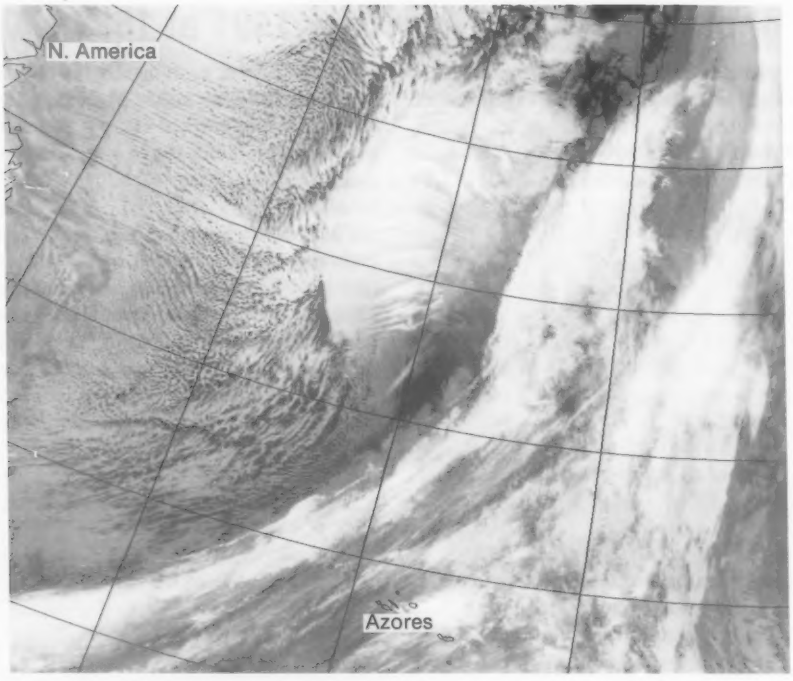

Figure 2. Infra-red image of the situation shown schematically in Fig. 1. *Photograph by courtesy of University of Dundee*

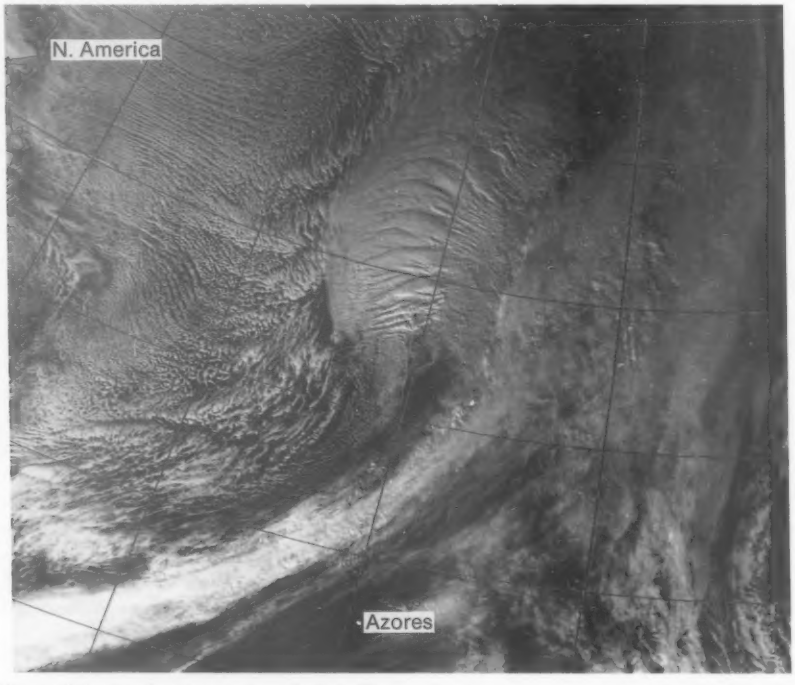

Figure 3. Visual image of the situation shown schematically in Fig. 1. *Photograph by courtesy of University of Dundee*

cater for the suspected existence of a much deeper depression. This successfully culminated in a much improved analysis, and a subsequent operational run of the model subsequently deepened the depression to 946 mb accompanied by an extremely vigorous circulation.

J. Norris and M.V.Young

GUIDE TO AUTHORS

Content

Articles on all aspects of meteorology are welcomed, particularly those which describe results of research in applied meteorology or the development of practical forecasting techniques.

Preparation and submission of articles

Articles, which must be in English, should be typed, double-spaced with wide margins, on one side only of A4-size paper. Tables, references and figure captions should be typed separately. Spelling should conform to the preferred spelling in the *Concise Oxford Dictionary* (latest edition). Articles prepared on floppy disk (Compucorp or IBM-compatible) can be labour-saving, but only a print-out should be submitted in the first instance.

References should be made using the Harvard system (author/date) and full details should be given at the end of the text. If a document is unpublished, details must be given of the library where it may be seen. Documents which are not available to enquirers must not be referred to, except by 'personal communication'.

Tables should be numbered consecutively using roman numerals and provided with headings.

Mathematical notation should be written with extreme care. Particular care should be taken to differentiate between Greek letters and Roman letters for which they could be mistaken. Double subscripts and superscripts should be avoided, as they are difficult to typeset and read. Notation should be kept as simple as possible. Guidance is given in BS 1991: Part 1: 1976, and *Quantities, Units and Symbols* published by the Royal Society. SI units, or units approved by the World Meteorological Organization, should be used.

Articles for publication and all other communications for the Editor should be addressed to: The Chief Executive, Meteorological Office, London Road, Bracknell, Berkshire RG12 2SZ and marked 'For Meteorological Magazine'.

Illustrations

Diagrams must be drawn clearly, preferably in ink, and should not contain any unnecessary or irrelevant details. Explanatory text should not appear on the diagram itself but in the caption. Captions should be typed on a separate sheet of paper and should, as far as possible, explain the meanings of the diagrams without the reader having to refer to the text. The sequential numbering should correspond with the sequential referrals in the text.

Sharp monochrome photographs on glossy paper are preferred; colour prints are acceptable but the use of colour is at the Editor's discretion.

Copyright

Authors should identify the holder of the copyright for their work when they first submit contributions.

Free copies

Three free copies of the magazine (one for a book review) are provided for authors of articles published in it. Separate offprints for each article are not provided.

Contributions: It is requested that all communications to the Editor and books for review be addressed to the Chief Executive, Meteorological Office, London Road, Bracknell, Berkshire RG12 2SZ, and marked 'For *Meteorological Magazine*'. Contributors are asked to comply with the guidelines given in the *Guide to authors* which appears on the inside back cover. The responsibility for facts and opinions expressed in the signed articles and letters published in *Meteorological Magazine* rests with their respective authors.

Back numbers: Full-size reprints of Vols 1–75 (1866–1940) are available from Johnson Reprint Co. Ltd, 24–28 Oval Road, London NW1 7DX. Complete volumes of *Meteorological Magazine* commencing with volume 54 are available on microfilm from University Microfilms International, 18 Bedford Row, London WC1R 4EJ. Information on microfiche issues is available from Kraus Microfiche, Rte 100, Milwood, NY 10546, USA.

June 1991

Edited by Corporate Communications
Editorial Board: R.J. Allam, R. Kershaw, W.H. Moores, P.R.S. Salter

Vol. 120
No. 1427

Contents

Page

An analysis of a 'wet' stack plume. F.B. Smith 97

The role of observations in climate prediction and research.
D.J. Carson 107

Awards
L.G. Groves Memorial Prizes and Awards for 1989 114

Correction 114

Satellite photographs — 2 February 1991 at 1533 UTC.
J. Norris and M.V. Young 115

ISSN 0026–1149

ISBN 0-11-728857-8

9 780117 288577